DIRECTIONALLY SOLIDIFIED Al_2O_3-$ME_3Al_5O_{12}$ (ME: Y, Er and Yb) EUTECTIC COATINGS FOR THERMOPHOTOVOLTAIC SYSTEMS

Patricia B. Oliete[a], Manuel J. López-Robledo[a,b], José I. Peña[a], Jorge Silva[a]

a) Instituto de Ciencia de Materiales de Aragón (ICMA), CSIC–Universidad de Zaragoza, E50018–Zaragoza, Spain.

b) Centro Universitario de la Defensa, General Military Academy, Ctra. Huesca s/n, E50090–Zaragoza, Spain

* Corresponding author: P.B. Oliete Tel: +34 876 555 605; Fax: +34 976 761 957

E-mail adresses: poliete@unizar.es (P.B. Oliete); robledo@unizar.es (M.J. Robledo); jipena@unizar.es (J.I. Peña); jsilva@unizar.es (J. Silva)

ABSTRACT

Selective emitters for thermophotovoltaic systems consisting of directionally solidified Al_2O_3-$ME_3Al_5O_{12}$ (ME: Y, Er and Yb) eutectic coatings on Al_2O_3 substrates were produced and characterizated. Coatings were deposited by dip-coating on cylindrical substrates. After sintering, a continuous-wave CO_2 laser was used to produce the surface resolidification. The optimization of the processing parameters yielded dense eutectic coatings with good adhesion to the substrate and with 90-200 μm in thickness. All coatings were free of voids and showed a eutectic microstructure consisting of a three dimensional interpenetrated network of Al_2O_3 and $ME_3Al_5O_{12}$. The mechanical properties of the coatings (hardness and fracture toughness) were evaluated by indentation techniques. Thermal emission was studied by heating the rods with a CO_2 laser at temperatures between 1000 and 1400 ºC. Selective emission was observed in

Er^{3+} and Yb^{3+} based coatings and attributed to the electronic transitions of the rare earth ions. Er^{3+}-coatings showed the best emission properties as selective emitters for thermophotovoltaic converters.

Keywords: laser remelting; $Al_2O_3/ME_3Al_5O_{12}$; eutectic coating; selective emitters; thermophotovoltaic converters

1. INTRODUCTION

Thermophotovoltaic systems (TPV) generate electricity from the electromagnetic radiation emitted by a body (emitter) at high temperature [1]. This radiation excites a photovoltaic cell that converts the photons in electrical energy. The emitter can be a blackbody/gray body, showing a broad continuous thermal emission, or a selective emitter, that is, a material emitting in a few emission bands. In order to increase the efficiency of the TPV converter, the selective emitter should emit in a spectral region coincident with the bangap of the photovoltaic cell [2].

Rare earth oxides are good candidates as selective emitters because they emit in narrow bands even when they are in high concentrations. Er^{3+} and Yb^{3+} are the most investigated rare earth ions for TPV as their narrow band emissions match with the sensible region of different photovoltaic cells [3-4].

As the selective emitter has to operate at temperatures above 800 ºC, the material should exhibit a good high-temperature microstructure and mechanical stability. Unfortunately, radiators fabricated using monolithic rare earth oxides are found to have low thermal shock resistance [5], cracking at temperatures of 1000 ºC. Recently, some investigations on selective emitters based in directionally solidified eutectic ceramics (DSEC) have been reported [6-9]. DSEC based in Al_2O_3 meet the thermostructural challenge required for TPV systems, due to their good creep resistance and microstructure stability [10-14], besides presenting selective emission when rare earth ions are incorporated to the eutectic. There are still very few studies on eutectic ceramics for TPV applications. Sai *et al.* [6] and Nakagawa *et al.* [7] have produced Al_2O_3-$Er_3Al_5O_{12}$ eutectic selective emitters compatible with a GaSb photovoltaic cell using the Bridgman technique. The processing with the laser-assisted floating zone

(LFZ) technique has allowed obtaining eutectic ceramics with finer microstructures and improved mechanical properties [8-9, 14].

Another alternative to the use of bulk oxide ceramics is the preparation of selective emitting coatings. Recently, it has been reported the fabrication of rare-earth based coatings with selective emission properties applied by plasma-spraying [15,16] or sol-gel process [17] on different refractory substrates. Coating thickness larger than 100 μm are needed to produce large emittance [4] and to neglect the emission of the substrate [16].

The aim of the present work is to fabricate Al_2O_3-$ME_3Al_5O_{12}$ (ME: Y, Er and Yb) eutectic ceramic coatings on Al_2O_3 substrates and to study the selective emission. Al_2O_3 will be an ideal substrate due to its excellent chemical and mechanical performance at high temperatures, to its low emittance and to the good matching of its thermal expansion coefficient with that of the eutectic ceramic coating, which will reduce the thermal stresses and provide a good response to thermal cycles. Layers with eutectic composition will be deposited by dip-coating and remelted using a CO_2 laser to enhance the performance of the coating [18,19]. The high temperature selective emission will be evaluated as a function of the composition of the eutectic.

2. MATERIALS AND METHODS

Directionally solidified eutectic coatings of Al_2O_3-$Y_3Al_5O_{12}$ (AY), Al_2O_3-$Er_3Al_5O_{12}$ (AE), and Al_2O_3-$Yb_3Al_5O_{12}$ (AYb) were fabricated using laser remelting. Commercial Al_2O_3 rods of 3 mm diameter and 50 mm length were used as substrate. Concentrated suspensions for dip-coating (solid loading of 20 vol.%) were prepared by mixing commercial powders of Al_2O_3 (Sasol, 99.99%), Y_2O_3 (Aldrich, 99.99%), Er_2O_3 (Alfa Aesar, 99.99%) or Yb_2O_3 (Alfa Aesar, 99.998%) in eutectic compositions (see

Table 1), solvents (ethanol), binder (polyvinyl butyral) and dispersant (phosphate ester). The cylindrical substrates were dipped in a range between 10-15 dips in the slurries and coated at a pulling rate of 4.5 mm/s. The coated films were dried in air and sintered between 1200 and 1500 ºC for 2-6 h in air.

After sintering, laser surface melting was performed in air using a continuous wave CO_2 laser. During the laser remelting process, CO_2-laser was focused annularly on the sample surface. Directionally solidified eutectic coatings were obtained by pulling the rod downwards at 200 mm/h with a rotation speed of 100 rpm and a laser power of 40-60 W.

Microstructural characterization was performed in polished transverse and longitudinal cross-sections of rods by means of back-scattered electron images obtained in a Scanning Electron Microscopy (SEM) (model 6400, Jeol, Tokyo, Japan) and a Field Emission SEM (model Carl Zeiss MERLIN). Specimens for this characterization were prepared using conventional metallographic methods.

The Vickers hardness on laser treated layers was measured following the ASTM C1327-99 Standard using a microhardness tester Matsuzawa, MXT 70, with an indentation load of 4.9 N and a holding time of 15 s. At least ten valid indentations were made on polished longitudinal cross sections. The fracture toughness was determined by the indentation technique. The crack lengths were measured using the optical microscope of the microhardness tester.

Thermal emission spectra were measured by heating the samples with the CO_2-laser used in the laser treatment. Emitted light was collected using an optic fibre and the emission spectrum was measured in the 900-2500 nm range using an NIR 256-2.5 from Ocean Optic spectrophotometer. The spectral sensitivity of the spectrometer was calibrated using a halogen lamp from Ocean Optics (Model HL-3P-CAL EXT).

Temperature of the sample was measured using a two-colour pyrometer (Impac, ISR12-LO MB33) and varied from 1000 to 1400 ºC by changing the laser power.

3. RESULTS AND DISCUSSION

3.1. Microstructure

AY, AE, and AYb eutectic layers were deposited by dip coating on Al_2O_3 rods and laser remelted. SEM micrograph analysis was used to study the coating microstructure and the adhesion to the substrate. Ceramic coatings obtained after 10-15 dips and sintered at high temperature had a thickness in a range of 150-300 μm. The laser remelting of the deposited layer produced a reduction around 30-40% in thickness.

Figure 1 shows the transverse-cross section of an AY layer on Al_2O_3 obtained by dip coating and sintered at 1500 ºC. A homogeneous layer of 175 μm in width was obtained, showing a good adhesion to the substrate.

Figure 2 shows SEM images of the transverse-cross section after directional solidification of the sintered layer. A dense, adherent, and free of voids coating can be observed in figure 2(a). Laser power used in the process produced only a partial remelting of the coating prepared by dip coating (Fig. 2(b)). For all the compositions, the remelted layer showed a eutectic microstructure consisting of a 3D interpenetrated network of both eutectic phases (Al_2O_3, black contrast, $ME_3Al_5O_{12}$, light contrast, with ME: Y, Yb or Er), as presented in figure 3. This type of microstructure, also known as Chinese script, has been reported in several Al_2O_3 -based eutectic ceramics [9-11]. The eutectic interspacing, measured from transverse-cross section SEM micrographs using the linear interception method, was of 0.69 ± 0.1 μm for AY, 0.71 ± 0.1 μm for AYb and 0.74 ± 0.1 μm for AE.

The depth of the remelted layer was strongly dependent on the laser power. Figure 4 shows the longitudinal cross sections of AY layers processed at different powers. At low power, (figure 4 (a)) only a partial laser remelting is observed in the coating. When increasing the power, the remelted coating layer was thicker, and a fully remelted layer of ~125 μm thick was obtained at 47 W (figure 4 (b)). At higher power (figure 4 (c)), the substrate close to the layer melted and coarse Al_2O_3 primary phase was found in the directionally solidified layer. Figure 4 (d) shows the region of the coating next to the substrate. A clean coating-substrate interface was found. We can also observe, in addition to the submicrometric eutectic microstructure presented in figure 3, a banding formed by coarsened Al_2O_3 and garnet phases. The presence of banding has been associated in the literature to instabilities in the melt produced by periodic perturbations [20]. In this case, the measured length between bands of 30-35 μm corresponds to the distance travelled by the rod in a revolution, indicating that the banding phenomenon observed in the coating is related to the rotation speed of the rod during the directional solidification.

Same results were obtained in AE and AYb coatings. Figure 5 (a) shows a detail of the transverse cross section of a directionally solidified AE coating of ~110 μm thick. A dense and free of voids coating was obtained. The excellent adhesion coating-substrate can be observed in Figure 5 (b).

3.2. Mechanical properties

Hardness, H, and fracture toughness, K_{IC}, of the remelted layers were determined at room temperature using a Vickers microhardness tester. Figure 6 shows the indentation fracture pattern in a remelted AYb coating. Well-defined, symmetric cracks

emerged from the indentation corners. Crack propagation was generally transgranular and the crack path was mainly straight, indicating a strong bonding between the eutectic phases (see inset in figure 6). Small cracks deflections in the interphases were observed in some cracks.

K_{IC} was determined by measuring the length of the cracks caused by the Vickers indentations. This method presents the advantages of simplicity and economy in addition to the small size of specimen. Although some works have recently revised the use of the indentation method for the absolute determination of the fracture toughness [21], this technique is suited to toughness evaluation on a comparative basis, as in the present study.

The evaluation of the fracture toughness from the indentation method can be performed using different equations depending of the type of cracks formed. Two major types of cracks can be developed, median-radial cracks and Palmqvist cracks. For all the eutectic coatings, the Niihara condition for median cracks ($c/a > 2.5$) [22] was fulfilled with c, the distance from the centre of the indentation to the crack tip and a, half diagonal of the Vickers indentation. The fracture toughness was calculated using the equation proposed by Anstis [23] for median cracks,

$$K_{IC} = 0.016\,(E/H)^{1/2}\,(P/c^{3/2}) \qquad (1)$$

where P is the indentation load, and E the Young modulus of the eutectic. An E-value of 340 GPa was taken for AY [13] and AYb and of 311 GPa for AE [24]. Table 2 lists the microhardness and fracture toughness obtained for AY, AE and AYb coatings. The values obtained are very similar in all the remelted layers and very close to those reported for directionally solidified AE and AY eutectic bulk [13, 24]

3.3. Selective thermal emission

Thermal emission of the eutectic coatings in the near infrared spectral region was measured from 1000 to 1400 ºC using a CO_2-laser as the heating source. Figures 7 (a), (b) and (c) show the thermal emission measured in the directionally solidified AY, AYb and AE coatings at different temperatures. Whereas AY spectrum consists in a weak, broad and structureless emission, the coatings containing rare earth ions present selective emission consisting of narrow lines in the 1-1.5 μm range. In the case of AE coating, an intense emission band centred at 1550 nm, matching with the GaSb photovoltaic cells, and a much weaker line at 980 nm were observed. For AYb coating only one emission band at 1000 nm was measured, compatible with a Silicon cell. The semiconductor band gaps are presented in the figures for comparison purposes.

The selective emissions in AE and AYb coatings were attributed to the radiative de-excitation of the rare-earth ion from the different excited states to the ground state. In particular, the observed measured emission bands in AE correspond to the $^4I_{13/2} \rightarrow {}^4I_{15/2}$ and $^4I_{11/2} \rightarrow {}^4I_{15/2}$ electronic transitions of Er^{3+} ions and in AYb to the $^2F_{5/2} \rightarrow {}^2F_{7/2}$ transition of Yb^{3+} ions, the only electronic transition available in this spectral region. Emission bands present some structure due to the degeneration removal of the ground and excited states of the rare-earth ions via the crystal field interaction.

The thermal excitation of the ions was assumed to occur by energy transfer from the lattice [25]. The selective emission becomes more intense with the temperature, as the thermal excitation of the rare-earth ions increases, the position and half-width of the lines remaining essentially the same with the temperature.

In addition to the narrow emission bands ascribed to the rare earth ions, we can observe a broad background, which can be attributed to lattice defects [26] and to the

substrate. This off-band emission in AE coating was almost negligible in all the range of temperatures showing a high selectivity even at 1400 ºC. However, the selectivity in AYb was significantly lower. We have to take into account that at this range of temperatures, the blackbody radiation at 1 μm is significantly less intense than at 1.5 μm and so, the peak to background ratio is expected to be lower in AYb than in AE.

In order to study the effect of laser remelting the deposited layer on the emission properties, the thermal emission of sintered AE coatings was also measured. The experiment was performed on a sample where only half the length was laser processed, the other half remaining only sintered. The optical fibre was fixed at ≈35 mm from the sample and the heated zone in the coating was selected by displacing the sample vertically. Figure 8 shows the thermal emission of the sintered AE coating and the corresponding laser remelted AE coating measured at 1100 ºC. We can observe that the emission bands are practically coincident in positions, widths and selectivity. However, the overall intensity is significantly higher in the laser treated layer. One of the causes of this result might be the higher light scattering expected in sintered AE coatings. In fact, some authors [27,28] calculated the effect of scattering in the spectral emittance of thin film dielectric materials and concluded that a large scattering albedo can account for a significant emittance reduction. The optimized eutectic microstructure obtained by directional solidification provides a lower scattering rate compared to sintered AE coatings and therefore, more thermal radiation is expected to be emitted in the direction where the optical fibre can collect it.

4. CONCLUSIONS

Novel cylinder selective emitters based on directionally solidified eutectic coatings have been investigated. AY, AYb and AE coatings have been deposited on Al_2O_3 substrates and directionally solidified using a CO_2 laser. The laser remelting of the deposited layer provided a dense, continuous, void-free and well-adhered coating with an interpenetrated eutectic microstructure for all the compositions.

The mechanical characterization at room temperature showed that the hardness and fracture toughness of the eutectic coatings reached similar values to those reported for the directionally solidified eutectic rods. Thermal emission of the eutectic coatings was measured as a function of the temperature. Selective emissions consisting of intense and narrow bands in the 1-1.5 μm range were observed in Er^{3+} and Yb^{3+} based coatings, being ascribed to the rare earth electronic transitions. The selectivity was dependent on the composition, erbium-based coatings showing higher peak to background ratio and high selectivity up to 1400 ºC. The excellent matching of the selective emission of the rare-earth ions with the sensitive region of some photovoltaic cells makes these coatings promising materials as TPV emitters.

ACKNOWLEDGEMENTS

The authors gratefully acknowledge the financial support from the Ministerio de Economía y Competitividad de España under project MAT2013-41045-R and from the Centro Universitario de la Defensa de Zaragoza under project UZCUD2014-TEC-11. Authors also acknowledge the use of Servicio de Microscopia Electrónica (Servicios de Apoyo a la Investigación), Universidad de Zaragoza.

REFERENCES

[1] T.J. Coutts, A review of progress in thermophotovoltaic generation of electricity, Renewable and Sustainable Energy Reviews 3 (1999) 77–184.

[2] A. Licciulli, D. Diso, G. Torsello, S.Tundo, A.Maffezzoli, M.Lomascolo, M. Mazzer, The challenge of high-performance selective emitters for thermophotovoltaic applications, Semicond. Sci. Technol.18 (2003) S174–S183.

[3] G.E. Guazzoni, High-Temperature Spectral Emittance of Oxides of Erbium, Samarium, Neodymium and Ytterbium, Appl. Spectr. 26 (1972) 60–65.

[4] D.L. Chubb, A.M.T. Pal, M.O. Patton, P.P. Jenkins, Rare Earth Doped High Temperature Ceramic Selective Emitters, J. Eur. Ceram. Soc. 19 (1999) 2551-2562.

[5] G.E. Guazzoni, E. Kittl, Cylindrical erbium oxide radiator structures for thermophotovoltaic generators, R & D Tech. Rep. ECOIM-4249. U. S. Army Electronics Command, Fort Monmouth, New Jersey (1974).

[6] H. Sai, H. Yugami, K. Nakamura, N. Nakagawa, H. Ohtsubo, S. Maruyama, Selective emission of $Al_2O_3/Er_3Al_5O_{12}$ eutectic composite for thermophotovoltaic generation of electricity, Jpn. J. Appl. Phys. 39 (2000) 1957–1961.

[7] N. Nakagawa, H. Ohtsubo, Y. Waku, H. Yugami, Thermal emission properties of $Al_2O_3/Er_3Al_5O_{12}$ eutectic ceramics, J. Eur. Ceram. Soc. 25 (2005) 1285–1291.

[8] M.C. Mesa, P.B. Oliete, R.I. Merino, V.M. Orera, Optical absorption and selective thermal emission in directionally solidified Al_2O_3-$Er_3Al_5O_{12}$ and Al_2O_3-$Er_3Al_5O_{12}$-ZrO_2 eutectics J. Eur. Ceram. 33 (2013) 2587–2596.

[9] P.B. Oliete, M.C. Mesa, R.I. Merino, V.M. Orera, Directionally solidified Al_2O_3-$Yb_3Al_5O_{12}$ eutectics for selective emitters, Sol. Energy Mater. Sol. Cells 144 (2016) 405–410.

[10] J. LLorca, V.M. Orera, Directionally-solidified eutectic ceramic oxides, Prog. Mat. Sci. 51 (2006) 711–809.

[11] Y. Waku, N. Nakagawa, T. Wakamoto, H. Ohtsubo, K. Shimizu, Y. Kohtoku, High-temperature strength and thermal stability of a unidirectionally solidified Al_2O_3/YAG eutectic composite, J. Mater. Sci. 33 (1998) 1217–1225.

[12] Y. Waku, N. Nakagawa, H. Ohtsubo, A. Mitani, K. Shimizu, Fracture and deformation behavior of melt-grown composites at very high temperature, J. Mater. Sci. 36 (2001) 1585–1594.

[13] J.Y. Pastor, J. LLorca, A. Salazar, P.B. Oliete, I. de Francisco, J.I. Peña, Mechanical Properties of Melt-Grown Alumina–Yttrium Aluminum Garnet Eutectics up to 1900 K, J. Am. Ceram. Soc. 88 (2005) 1488–1495.

[14] M.C. Mesa, P.B. Oliete, J.Y. Pastor, A. Martín, J. LLorca, Mechanical properties up to 1900 K of $Al_2O_3/Er_3Al_5O_{12}/ZrO_2$ eutectic ceramics grown by the laser floating zone method, J. Eur. Ceram. Soc. 34 (2014) 2081-2087.

[15] W.J. Tobler, W. Durisch, Plasma-spray coated rare-earth oxides on molybdenum disilicide-high temperature stable emitters for thermophotovoltaics, Appl. Energy 854 (2008) 371–383.

[16] H.J. Wang, H. Ye, Y.Z. Zhang, Preparation and performance evaluation of Er_2O_3 coating-type selective emitter, Sci. China Tech. Sci. 57 (2014) 332□338.

[17] A. Licciulli, A. Maffezzoli, D. Diso, M. Mazzer, G. Torsello, S. Tundo, Porous garnet coating tailoring the emissivity of thermostructural materials, J. Sol-Gel Sci. Tech. 32 (2004) 247–251.

[18] A. Cubero, J.I. Peña, M.A. Laguna-Bercero, Optimization of Ni–YSZ solid oxide fuel cell anodes by surface laser melting, Appl. Surf. Sci. 335 (2015) 39–43.

[19] M. Szkodo, A. Bien, M. Antoszkiewicz, Effect of plasma sprayed and laser re-melted Al_2O_3 coatings on hardness and wear properties of stainless steel. 42 (2016) 11275-11284.

[20] J. LLorca, J.Y. Pastor, P. Poza, J.I. Peña, I. de Francisco, A. Larrea, V.M. Orera, Influence of the Y_2O_3 content and temperature on the mechanical properties of melt-grown Al_2O_3–ZrO_2 eutectics, J. Am. Ceram. Soc. 87 (2004) 633–639.

[21] G.D. Quinn, R.C. Bradt, On the Vickers indentation fracture toughness test, J. Am Ceram. Soc. 90 (2007) 673–680.

[22] K. Niihara, R. Morena, D.P.H. Hasselman, Evaluation of K_{IC} of brittle solids by the indentation method with low crack-to-indent ratios, J. Mater. Sci. Lett. 1 (1982) 13–16.

[23] G.R. Anstis, P. Chantikul, B.R. Lawn, D.B. Marshall, A critical evaluation of indentation techniques for measuring fracture toughness: I direct crack measurements, J. Am. Ceram. Soc. 64 (1981) 533–538.

[24] M.C. Mesa, P.B. Oliete, V.M. Orera, J.Y. Pastor, A. Martín, J. LLorca, Microstructure and mechanical properties of $Al_2O_3/Er_3Al_5O_{12}$ eutectic rods grown by the laser-heated floating zone method, J. Eur. Ceram. 31 (2011) 1241–1250.

[25] V.V. Golovlev, C.H. Winston Chen, W.R. Garrett, Heat to light energy conversion by emitters doped with rare-earth metal ions, Appl. Phys. Lett. 69 (1996) 280-282.

[26] R.E. Nelson, Thermophotovoltaic emitter development, AIP Conf. Proc. 321 (1995) 80-95.

[27] R.A. Lowe, D.L. Chubb, S.C. Farmer, B.S. Good, Rare-earth garnet selective emitter, App. Phys. Lett. 64 (1994) 3551-3553.

[28] C.R. Parent, R.E. Nelson, Thermophotovoltaic energy conversion with a novel rare earth oxide emitter, In Proceedings of the 21st Intersociety Energy Conversion. American Chemical Society*, Washington, DC*, 2, (1986) 1314-1317.

FIGURE CAPTIONS

Figure 1: (a) Back-scattered scanning electron micrograph of the transverse cross section of AY layer on Al_2O_3 obtained by dip coating and sintered at 1500 ºC. (b) Detail of the sintered layer.

Figure 2: (a) Back-scattered scanning electron micrograph of the transverse cross section of the directionally solidified AY eutectic coating on Al_2O_3 rod. (b) Detail of the partially remelted layer.

Figure 3: Back-scattered scanning electron micrograph of the transverse section of laser remelted AYb eutectic coating showing the interpenetrating network of Al_2O_3 (black) and $Yb_3Al_5O_{12}$ (white) eutectic phases.

Figure 4: Back-scattered scanning electron micrograph of the longitudinal cross section of laser remelted AY eutectic coating on Al_2O_3 rod at different laser power (a) 41 W, (b) 47 W and (c) 56 W. (d) Detail of the coating-substrate interface in the fully remelted layer.

Figure 5: (a) Back-scattered scanning electron micrograph of the transverse section of laser remelted AE eutectic coating on Al_2O_3 rod. (b) Detail of the coating-substrate interface.

Figure 6: Secondary electron micrograph showing the cracking pattern of laser remelted AYb eutectic coating under an indentation load of 4.9 N. Inset: Detail of the crack propagation.

Figure 7: Selective emission spectra of laser remelted (a) AY, (b) AYb and (c) AE eutectic coatings on Al_2O_3 measured at several temperatures. Bandgaps of silicon and GaSb are also presented for comparison purposes.

Figure 8: Selective emission spectra of a laser remelted AE coating (solid line) and a sintered AE coating (dotted line) at 1100 ºC.

Table 1: Eutectic composition of the samples.

Sample	AY	AE	AYb
Composition	81.5% mol Al_2O_3 18.5% mol Y_2O_3	81% mol Al_2O_3 19% mol Er_2O_3	81.5% mol Al_2O_3 18.5% mol Yb_2O_3

Table 2: Hardness (HV) and fracture toughness (K_{IC}) of AY, AE and AYb eutectic coatings and bulk values from [1] Ref. [13] and [2] Ref. [24].

	AY coating	AE coating	AYb coating	AY bulk[1]	AE bulk[2]
HV (GPa)	14.5 ± 0.4	14.9 ± 0.7	14.8 ± 0.6	14.8-16.3	14.4 -16
K_{IC} (MPa·$m^{1/2}$)	1.9 ± 0.3	1.8 ± 0.3	2.2 ± 0.5	2-2.2	1.7-2

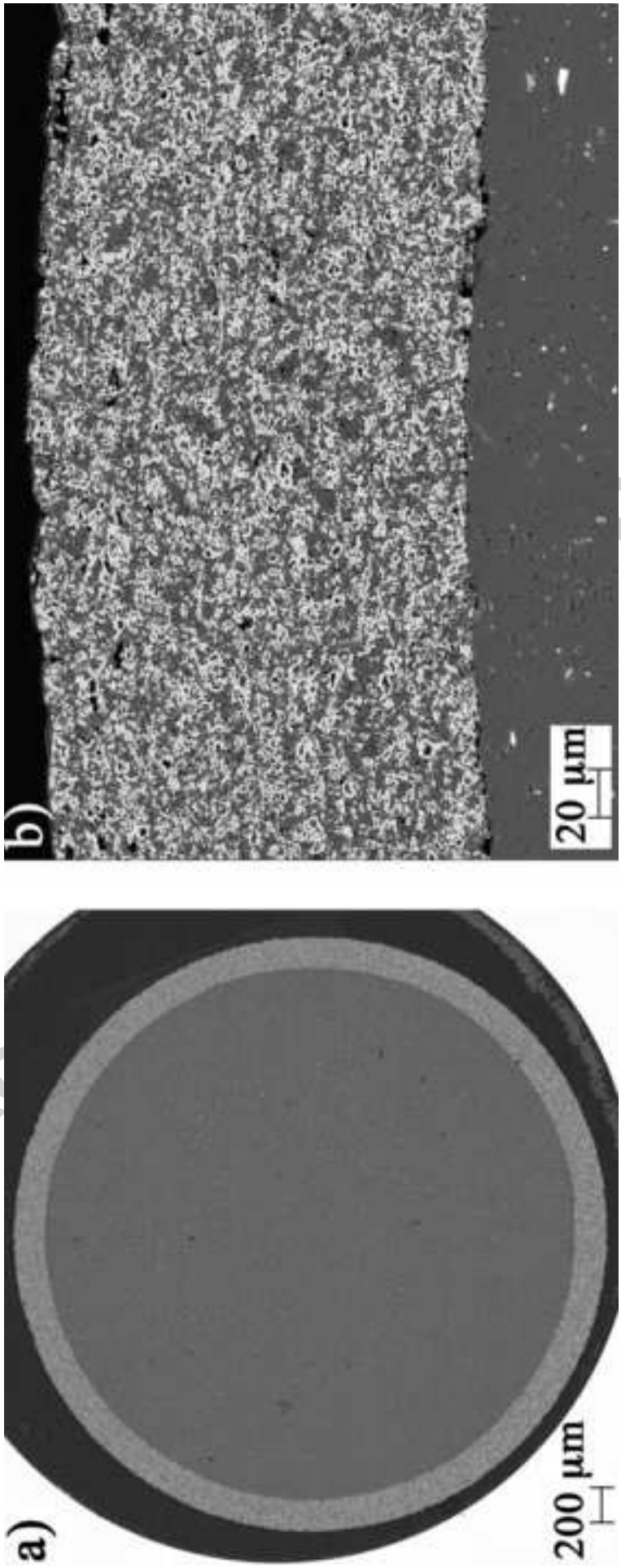

Figure 1

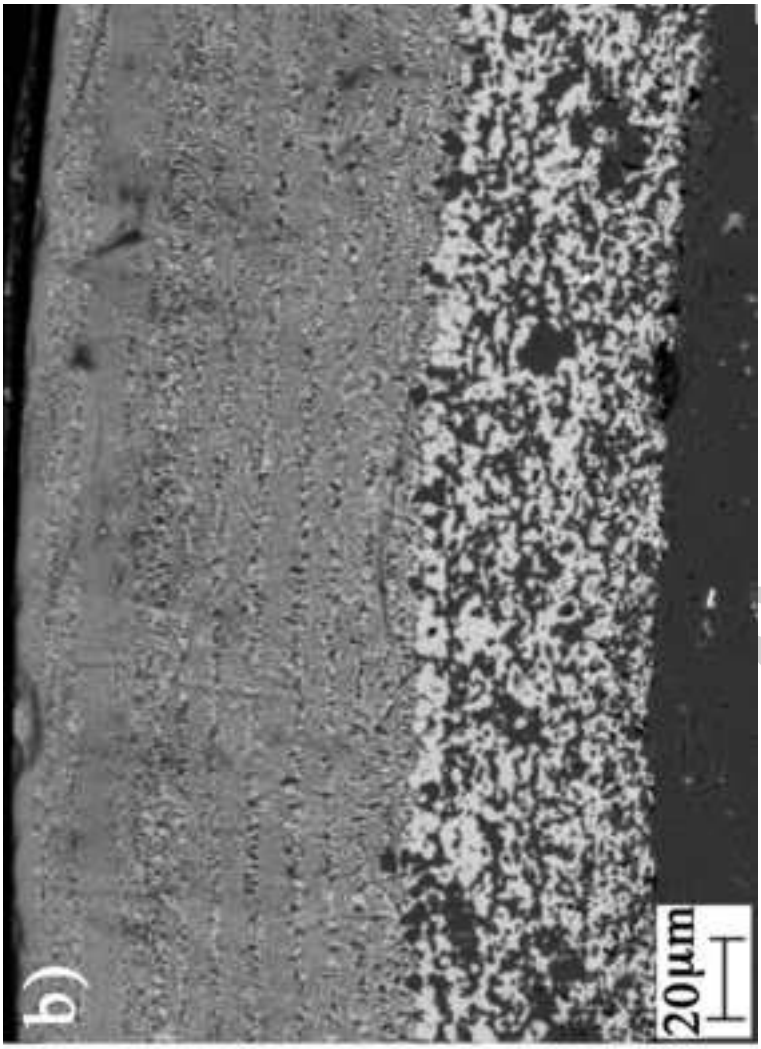

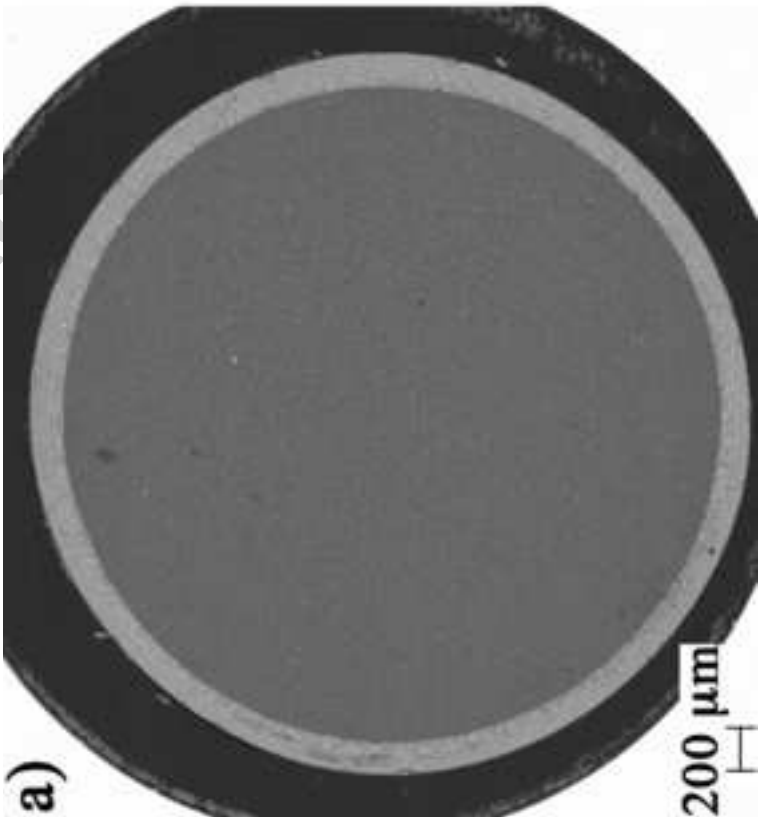

Figure 2

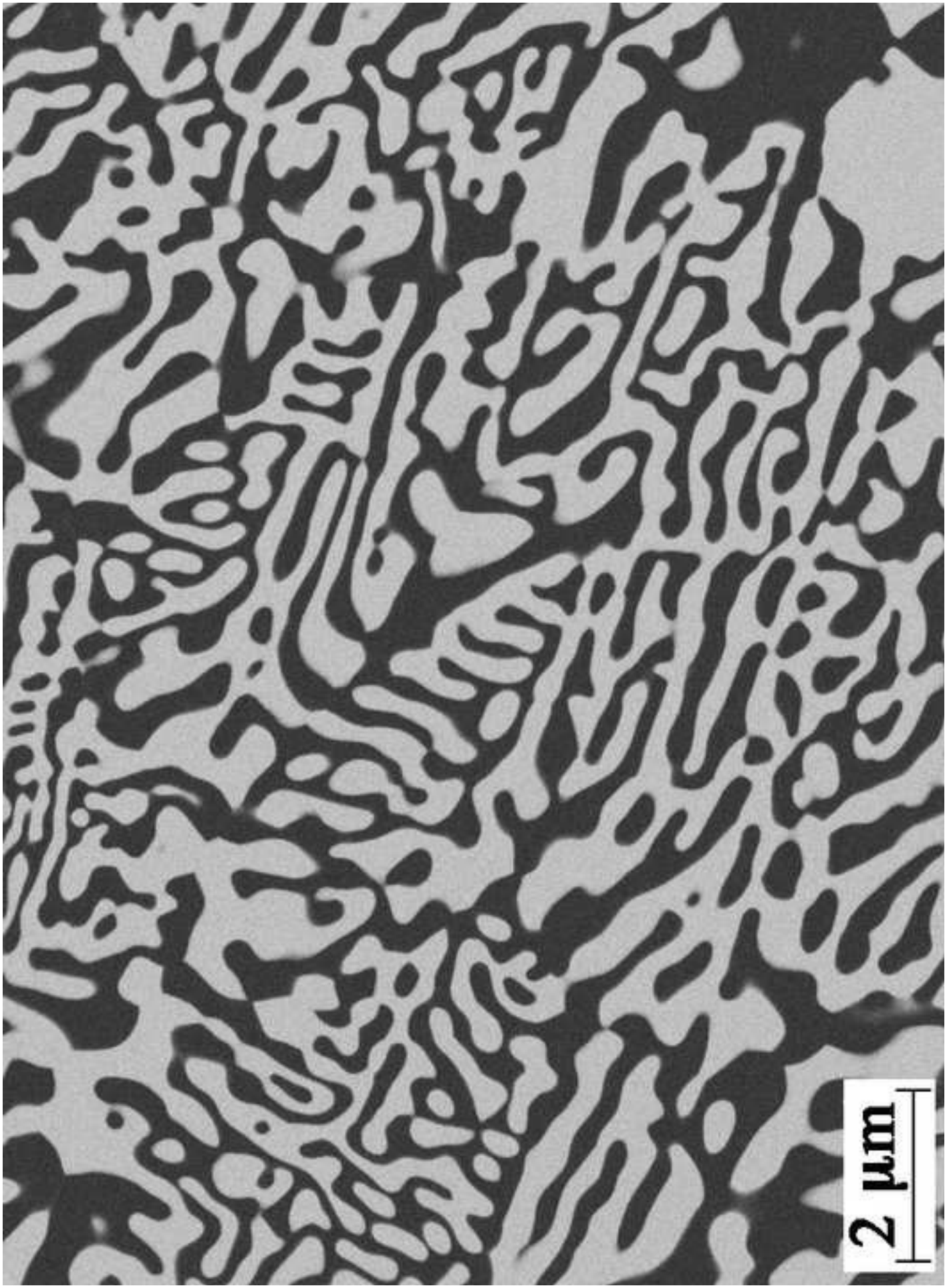

Figure 3

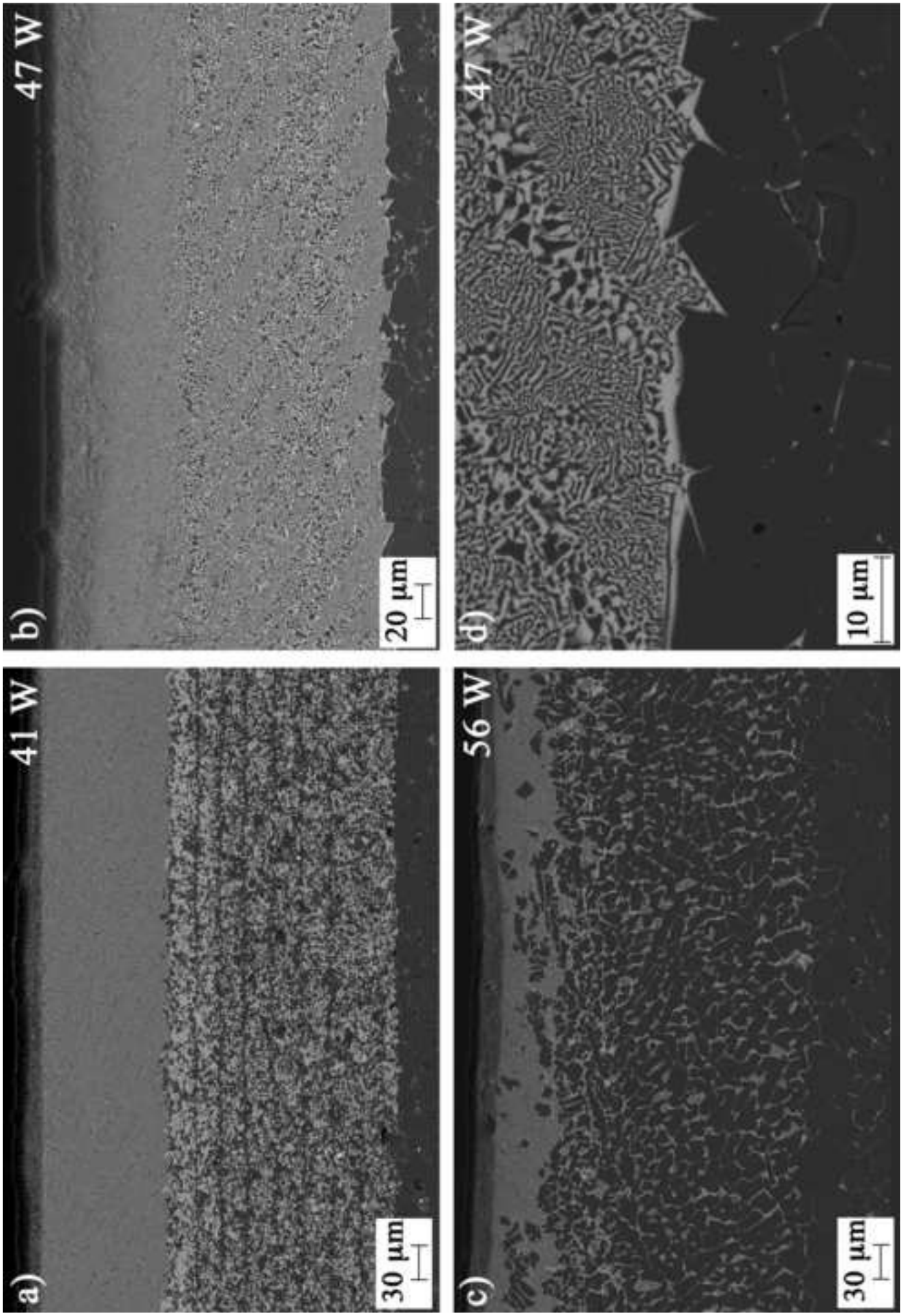

Figure 4

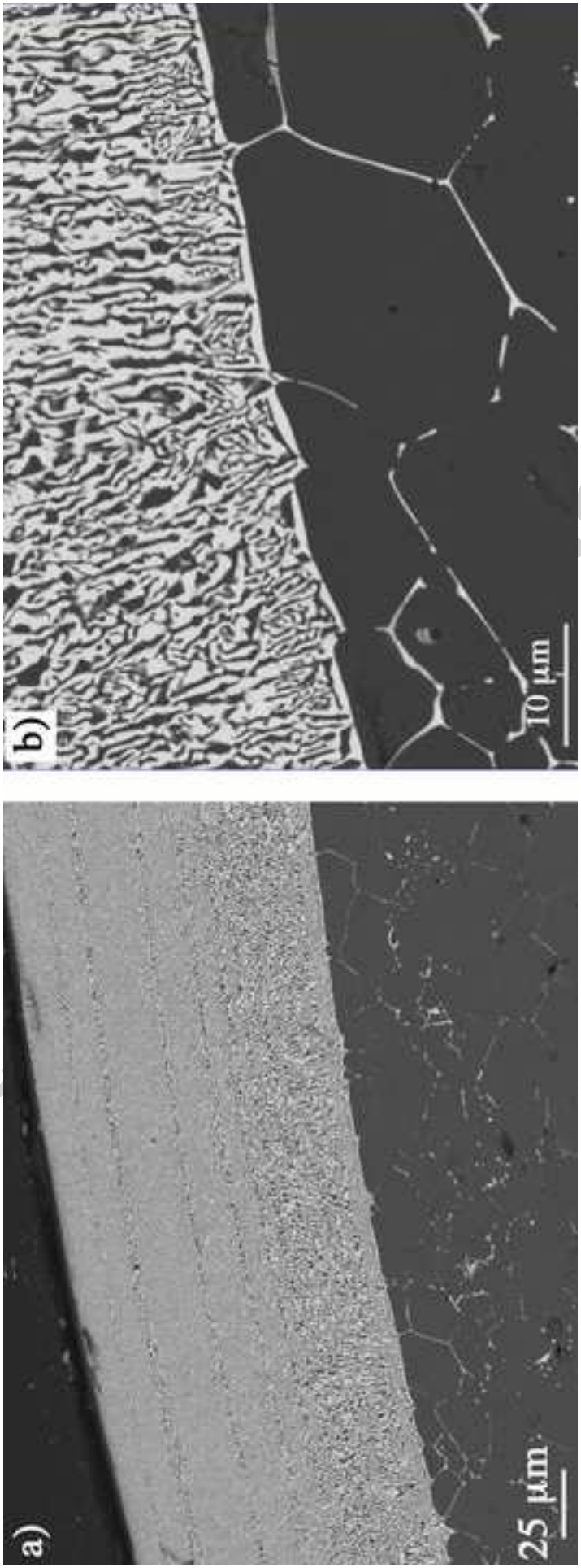

Figure 5

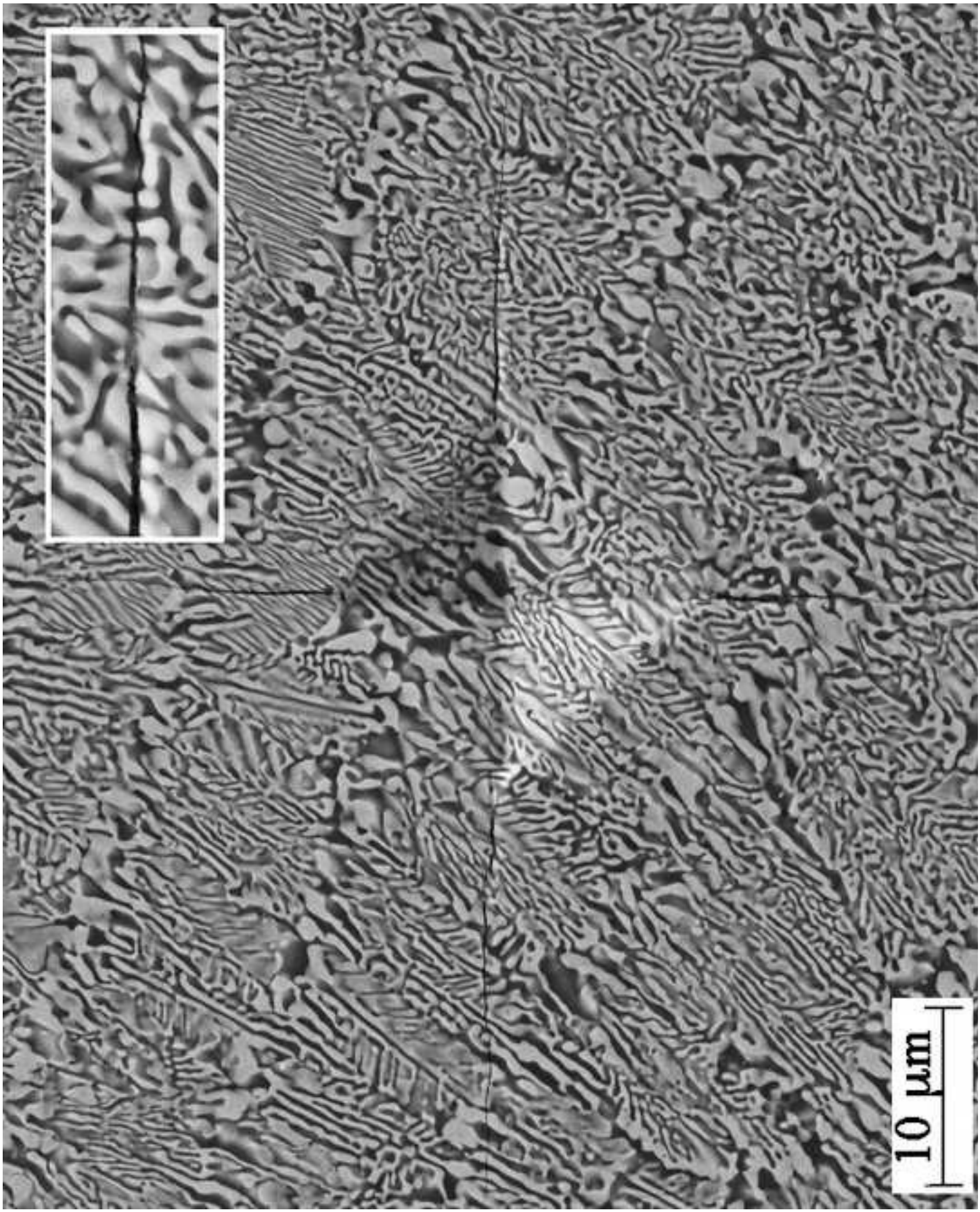

Figure 6

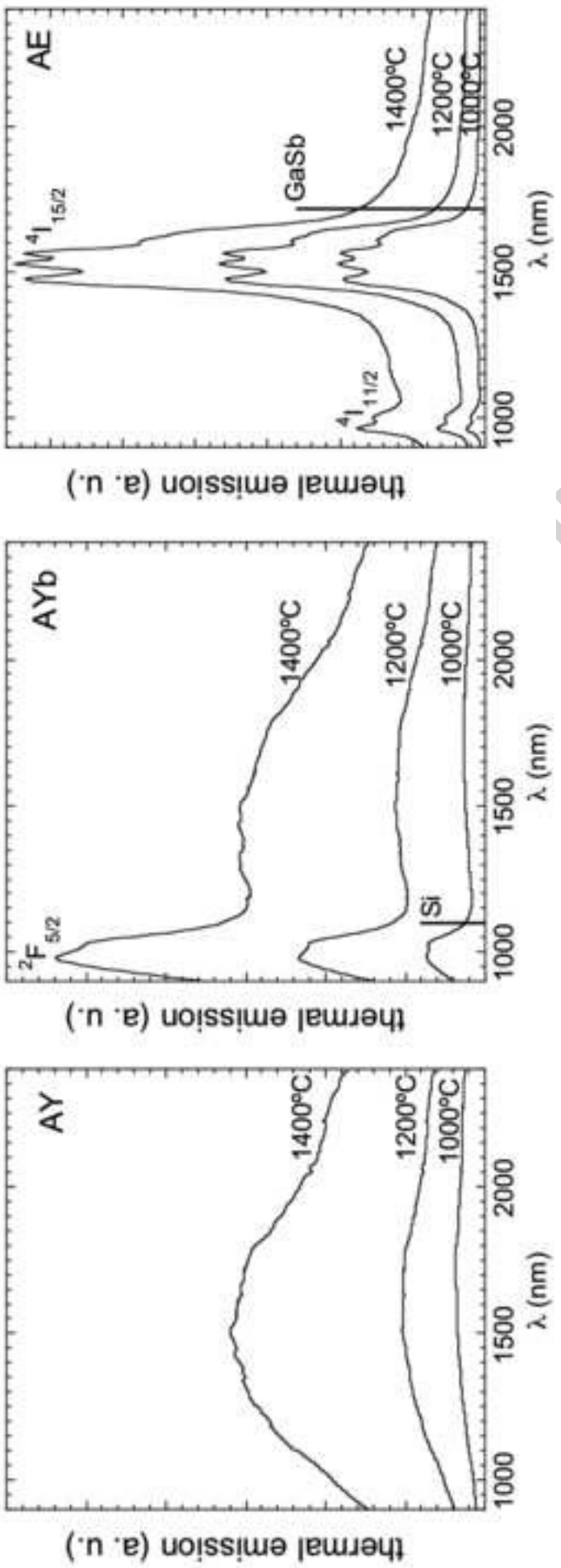
AE
$^4I_{15/2}$
$^4I_{11/2}$
GaSb
1400°C
1200°C
1000°C
thermal emission (a. u.)
λ (nm)
1000
1500
2000
AYb
$^2F_{5/2}$
Si
1400°C
1200°C
1000°C
thermal emission (a. u.)
λ (nm)
1000
1500
2000
AY
1400°C
1200°C
1000°C
thermal emission (a. u.)
λ (nm)
1000
1500
2000

Figure 7

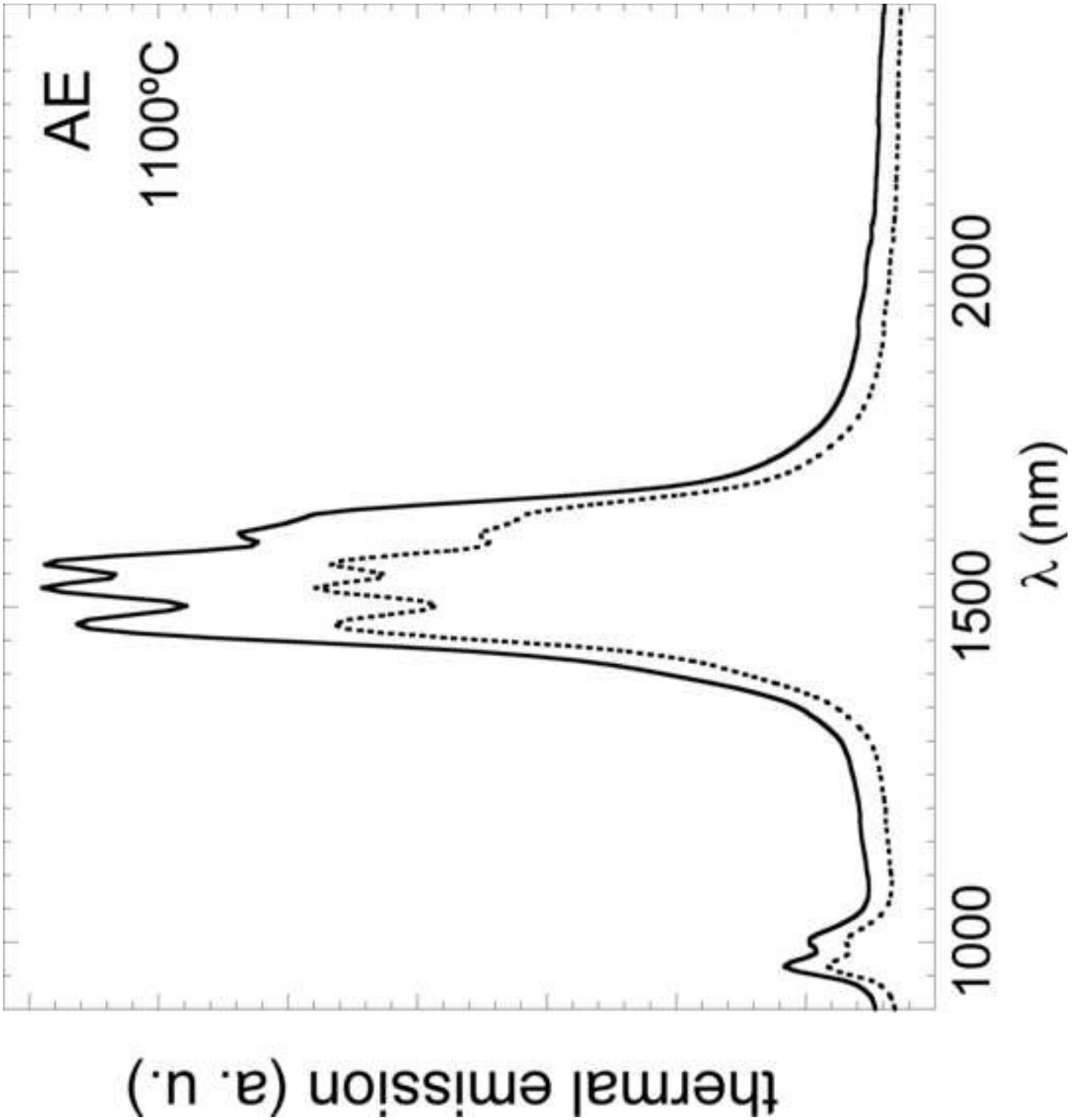

Figure 8